

# The Dynamic Interactions and Control of Long Slender Continua and Discrete Inertial Components in Vertical Transportation Systems

Stefan Kaczmarczyk

**Abstract** Dynamic phenomena such as transient and steady-state resonant vibrations in vertical transportation systems deployed to move goods and passengers in the modern built environment affect the performance of the entire installation. In extreme high rise structures traction drive elevator systems comprise long slender continua such as ropes and cables with discrete mass elements that exhibit low-frequency modes and nonlinear modal interactions. This results in the need to predict and control their non-linear stationary and non-stationary dynamic responses. The underlying causes of these dynamic responses / vibrations are varied. They include low frequency sway motions of the host structure induced by high winds and seismic activities. Consequently, conditions for external, parametric and autoparametric resonances can readily arise during the operation of such installations. In this context, a general approach to model the dynamic behaviour of a typical vertical transportation system is demonstrated. Subsequently, a mathematical model is developed which is solved numerically to predict the non-stationary / nonlinear dynamic responses. An active control strategy is then proposed to minimize the effects of adverse dynamic responses of the system.

## 1 Introduction

The design and operation of high-performance systems for vertical transportation in the modern built environment present many technical challenges due to adverse dynamic responses that arise due to various sources of excitation present in these systems. In the modern high-rise built environment excitations induced by winds and earthquake/ground motion can result in large responses of buildings and civil structures [1,2]. The dynamic responses at low frequencies and large amplitudes then arise that induce complex resonance interactions affecting the performance of vertical transportation systems (VTS) deployed in tall structures [3,4,5]. Passive and active control strategies can then be applied to mitigate their effects [6,7].

In this work a mathematical model to predict and to analyse the resonance behaviour of the tall host structure – VTS is presented. The VTS is equipped with a nonlinear damper / actuator ‘tie-down’ device. The performance of the installation is studied by numerical simulation. It is shown that the characteristics of the tie-down device can be

---

S. Kaczmarczyk  
The University of Northampton, University Drive, Northampton NN1 5PH, UK  
e-mail: stefan.kaczmarczyk@northampton.ac.uk

adjusted to minimize the effects of adverse dynamic responses of the system. The active stiffness strategy is then proposed to minimize the effects of adverse dynamic responses of suspension and compensating ropes in VTS.

## 2 Mathematical Model

A VT system may be considered as an assemblage of axially moving elastic one-dimensional long slender continua (LSC) divided into  $p = 1, 2, \dots, P$  sections of *slowly* varying length [8,9], constrained by discrete elements such as rigid-body masses and rotating inertia elements. Its response can be described by a system of nonlinear partial differential equations of the following form

$$\rho_s(x_p) \mathbf{U}_{,tt}^p + \mathbf{C}^p[\mathbf{U}_{,t}^p] + \mathbf{L}^p[\mathbf{U}^p] = \mathbf{N}^p[\mathbf{U}] + \mathbf{F}^p(x_p, t, \theta_p), \quad x_p \in \{0 < x_p < L_p(\tau)\}, \quad 0 \leq t < \infty, \quad (1)$$

where the boundary conditions are given as

$$\mathbf{B}_1^p(\mathbf{U}^p) = 0 \text{ at } x_p = 0, \quad \mathbf{B}_2^p(\mathbf{U}^p) = 0 \text{ at } x_p = L_p(\tau) \quad (2)$$

where  $x_p$  denotes the spatial co-ordinate,  $\mathbf{U}^p(x_p, t) = [U_1^p(x_p, t), U_2^p(x_p, t), U_3^p(x_p, t)]$  is a local (component) dynamic displacement vector representing motion of the component  $p$  in the lateral and longitudinal directions,  $(\cdot)_{,t}$  designates partial derivatives with respect to time  $t$ ,  $\tau = \varepsilon t$  represents the slow time scale, where  $\varepsilon$  is a small parameter [9], and  $\mathbf{C}^p$  and  $\mathbf{L}^p$  are local linear operators. Furthermore,  $\mathbf{N}^p$  is an operator acting upon the global displacement vector  $\mathbf{U}$ , and representing non-linear couplings and inter-component constraints in the system.  $\mathbf{F}^p$  is a forcing function with harmonic terms of frequency  $\dot{\theta}_p = \Omega_p$ , where the overdot indicates total differentiation with respect to time. The local (component) mass distribution function is defined as

$$\rho_p(x_p) = m_p + \sum_{i=1}^{N_M} M_i \delta(x_p - L_p) \quad (3)$$

In the model given by Eq. 1 the Lagrangian coordinates or Eulerian coordinates may be applied as the spatial coordinate  $x_p$ . If the Lagrangian formulation is applied, then it is convenient to refer the dynamic elastic deformations of LSC to a moving frame associated with the overall axial transport motion of the system [9]. Otherwise, a fixed (inertial) frame is used to describe the deformations. In order to discretize the continuous slowly varying nonlinear system Eq. 1 the following expansion can be used

$$U_k^p(x_p, t) = \sum_{n=1}^{N_p} Y_n^k(x_p; L_p(\tau)) q_n^p(t) \quad (4)$$

where  $Y_n^k(x_p; L_p(\tau))$  is the  $n$ th eigenfunction of the corresponding linear system and  $q_n^p(t)$  represent the  $n$ th modal coordinate. This expansion leads to the following first-order ordinary differential equation (ODE) system given as

$$\dot{\mathbf{y}}(t) = \mathbf{A}(t, \tau)\mathbf{y}(t) + \tilde{\mathbf{N}}(\tau, \mathbf{y}) + \tilde{\mathbf{F}}(t, \tau) \quad (5)$$

where  $\mathbf{y}$  is the system state vector,  $\mathbf{A}$  is a slowly varying linear coefficient matrix,  $\tilde{\mathbf{N}}$  is a vector function which represents the non-linear coupling terms, and  $\tilde{\mathbf{F}}$  is the external excitation vector. This system cannot be solved exactly. An approximate solution can be sought using asymptotic (perturbation) methods and/or numerical techniques. Alternatively, in some cases, the system of partial differential equations Eq. 1 with the boundary conditions given by Eq. 2 can be treated directly without discretization and perturbations methods (such as the method of multiple scales) can be applied to investigate the non-stationary behaviour of the system [10,11,12,13].

### 3 Vertical Transportation System – Traction Drive Elevator

In the modern high-rise built environment high-speed high-capacity traction drive elevator (lift) systems are used. A diagram which illustrates the dynamic model of a high-rise lift system is shown in Fig. 1. The modulus of elasticity, cross-sectional effective area and mass per unit length of the ropes are denoted as  $E_1$ ,  $A_1$ ,  $m_1$  and  $E_2$ ,  $A_2$ ,  $m_2$  for the compensating cables and the suspension ropes, respectively. The compensating cables are of length  $L_1$  at the car side and the suspension ropes are of length  $L_2$  at the counterweight side, respectively. The length of the suspension rope at the car side and the compensating rope at the counterweight side are denoted as  $L_3$  and  $L_4$ , respectively. The lengths of suspension ropes and compensating cables are varying with the position of the car in the shaft (denoted by  $l_{car}$ ). The masses and dynamic displacements of the car, counterweight and the compensating sheave assembly are represented by  $M_{car}$ ,  $M_{cwt}$  and  $M_{comp}$ ,  $q_1$ ,  $q_2$  and  $q_3$ , respectively. The compensating sheave rotational motion is represented by the angular coordinate  $\theta$  and the second moment of inertia is  $I_{comp}$ . The compensating sheave assembly (CSA) is equipped with a damper/ tie-down device. The building structure sway deformations due to ground motions  $s_v(t)$ ,  $s_w(t)$  are represented by the shape function  $\Psi(\eta) = 3\eta^2 - 2\eta^3$ ,  $\eta = z/Z_0$ . Consider that the ground motions are harmonic of frequency  $\Omega_1$ ,  $\Omega_2$  in the in-plane direction and out-of-plane direction, respectively. The deformations then result in harmonic motions  $v_0(t)$  and  $w_0(t)$  at the top of the building structure, in the in-plane direction and out-of-plane direction, respectively.

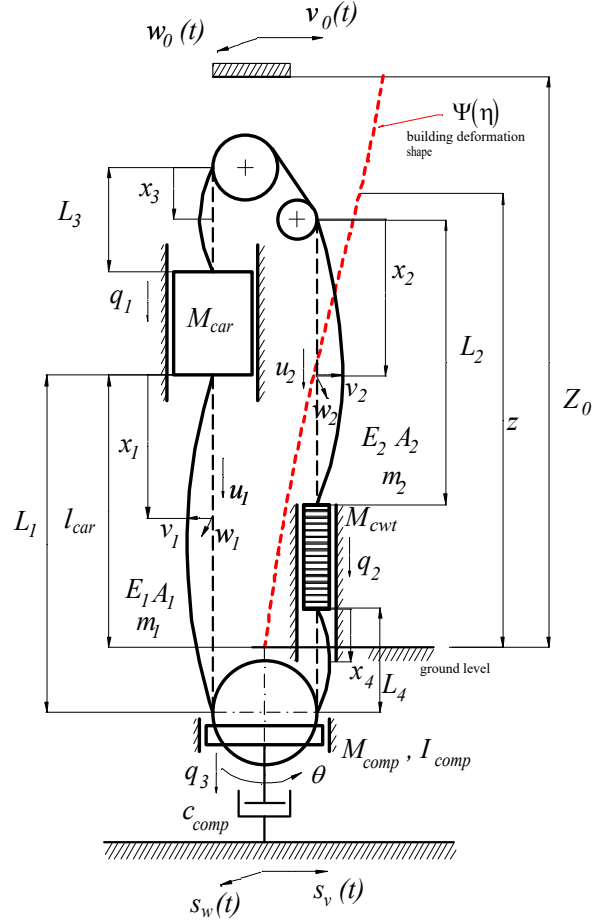


**Fig. 1. Model of a high-rise VTS**

The natural frequencies of the system change with the position of the car. An adverse situation arises when the building sways at its fundamental natural frequency which in turn is tuned to the natural frequency of the VTS, thus leading to resonance conditions. The resonance phenomena can be captured by the development of a suitable dynamic model. The model based on the formulation given in Eq. 1 is represented by Eq. 6, where  $V$ ,  $a$  represent the speed and acceleration/deceleration of the car,  $\bar{v}_i(x_i, t)$ ,  $\bar{w}_i(x_i, t)$ ,  $i = 1, 2, \dots, 4$ , represent the dynamic displacements of the ropes,  $T_i$ , denote the rope quasi-static tension terms.

$$\begin{aligned}
m_i \ddot{\bar{v}}_{itt} - \left\{ T_i - m_i \left[ V^2 + (g - a_i) x_i \right] + E_i A_i e_i \right\} \bar{v}_{ixx} + m_i g \bar{v}_{ix} + 2m_i V \bar{v}_{ixt} &= F_i^v \left[ t, L_i(t) \right], \\
m_i \ddot{\bar{w}}_{itt} - \left\{ T_i - m_i \left[ V^2 + (g - a_i) x_i \right] + E_i A_i e_i \right\} \bar{w}_{ixx} + m_i g \bar{w}_{ix} + 2m_i V \bar{w}_{ixt} &= F_i^w \left[ t, L_i(t) \right], \\
M_{car} \ddot{q}_1 - E_1 A_1 e_1 + E_2 A_2 e_3 &= 0, \\
M_{cwt} \ddot{q}_2 - E_1 A_1 e_4 + E_2 A_2 e_2 &= 0, \\
M_{comp} \ddot{q}_3 + E_1 A_1 e_1 + E_1 A_1 e_4 + F_d &= 0, \\
I_{comp} \ddot{\theta} - R E_1 A_1 e_1 + R E_1 A_1 e_4 &= 0,
\end{aligned} \tag{6}$$

where  $m_3 = m_2$ ,  $m_4 = m_1$ ,  $a_1 = a$ ,  $a_2 = -a$ ,  $a_3 = a$ ,  $a_4 = a$ ,  $E_3 A_3 = E_2 A_2$ ,  $E_4 A_4 = E_1 A_1$  and  $e_i$  denote the quasi-static axial strains in the ropes and are given as

$$\begin{aligned}
e_1 &= \frac{l}{L_1(t)} \left[ u_1(L_1, t) - q_1(t) + \frac{l}{2} \int_0^{L_1} (\bar{v}_{1x}^2 + \bar{w}_{1x}^2) dx_1 + \frac{\Psi_1^2}{2L_1(t)} (v_0^2 + w_0^2) \right], \\
e_2 &= \frac{l}{L_2(t)} \left[ q_2(t) + \frac{l}{2} \int_0^{L_2} (\bar{v}_{2x}^2 + \bar{w}_{2x}^2) dx_2 + \frac{(\Psi_h - \Psi_2)^2}{2L_2(t)} (v_0^2 + w_0^2) \right], \\
e_3 &= \frac{l}{L_3(t)} \left[ q_1(t) + \frac{l}{2} \int_0^{L_3} (\bar{v}_{3x}^2 + \bar{w}_{3x}^2) dx_3 + \frac{(\Psi_{car} - \Psi_{mach})^2}{2L_3(t)} (v_0^2 + w_0^2) \right], \\
e_4 &= \frac{l}{L_4(t)} \left[ u_4(L_4, t) - q_2(t) + \frac{l}{2} \int_0^{L_4} (\bar{v}_{4x}^2 + \bar{w}_{4x}^2) dx_4 + \frac{\Psi_{cwt}^2}{2L_4(t)} (v_0^2 + w_0^2) \right],
\end{aligned} \tag{7}$$

where the constraint  $2q_3 - u_1 - u_4 = 0$  needs to be applied and the force  $F_d$  given as

$$F_d = c_{comp} \dot{q}_3 |\dot{q}_3|^{\alpha-1}, \quad 0 < \alpha \leq 1 \tag{8}$$

is the damping force provided by the hydraulic tie-down of the damping coefficient  $c_{comp}$ .

## 4 The Dynamic Behaviour and Numerical Results

The dynamic responses of the system can be determined by solving the nonlinear set of partial differential equations (PDE) given by Eq. 6. In this study the dynamic interactions when the frequency of the building is tuned to the natural frequencies of the VT system are investigated.

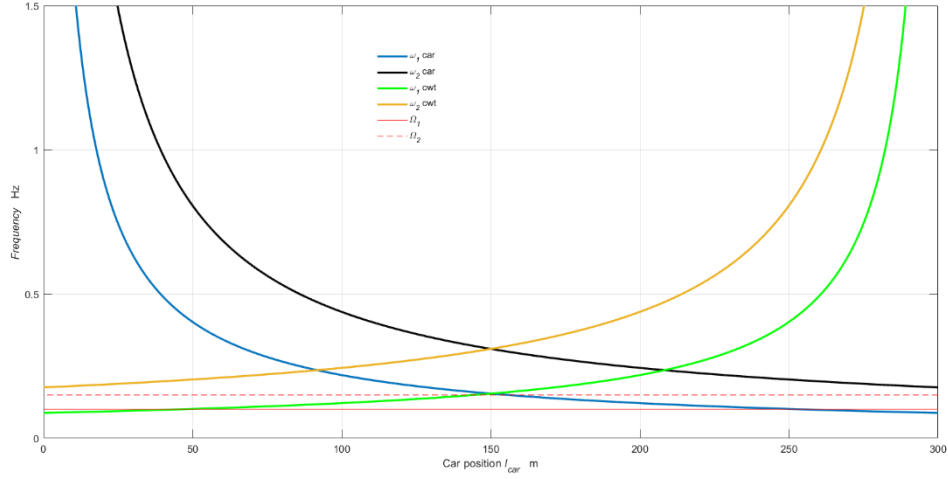


**Fig. 2** The natural frequencies – compensating cable lateral modes

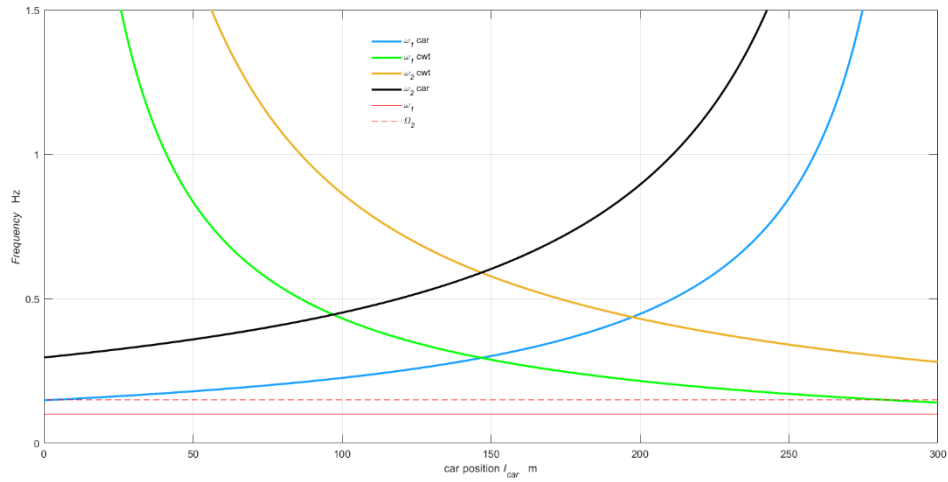


**Fig. 3** The natural frequencies – suspension rope lateral modes

Figs 2-4 show the variation of the natural frequencies of a VTS comprising a car of mass 5500 kg which carries rated load of 3000 kg. The travel height is 300 m and the installation is equipped with compensating ropes with a synthetic fiber core (SFC) of diameter 36 mm and mass per unit length  $m_{cr} = 4.76$  kg/m each. The CSA mass is 4500 kg. The car and counterweight (balanced at 50%) are suspended on 9-stranded steel core ropes of diameter 19 mm and mass per unit length  $m_{sr} = 1.54$  kg/m each. The horizontal (bending mode) natural frequencies of the building structure are given as  $\Omega_1 = 0.1$  Hz in the in-plane direction and  $\Omega_2 = 0.15$  Hz in the out-of-plane direction, respectively. The frequency curves are plotted against the position of the car in the shaft

(measured from the bottom landing level), with the in-plane and out-of-plane excitation frequencies represented by red solid/ dashed horizontal lines, respectively. It is evident that in this arrangement primary resonance interactions within the suspension/ compensating system involve the lateral modes of the ropes. On the other hand the frequencies of vertical mode are much higher than the frequencies of the building.

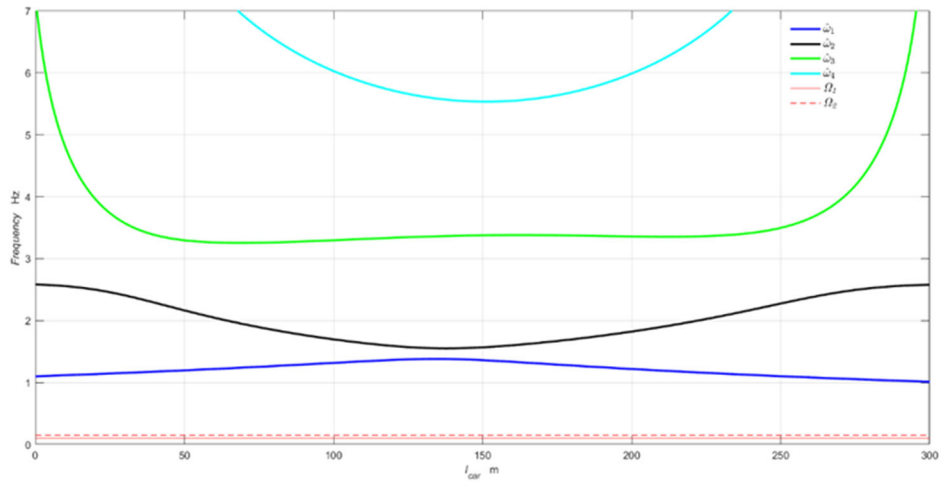


**Fig. 4** The natural frequencies – vertical modes

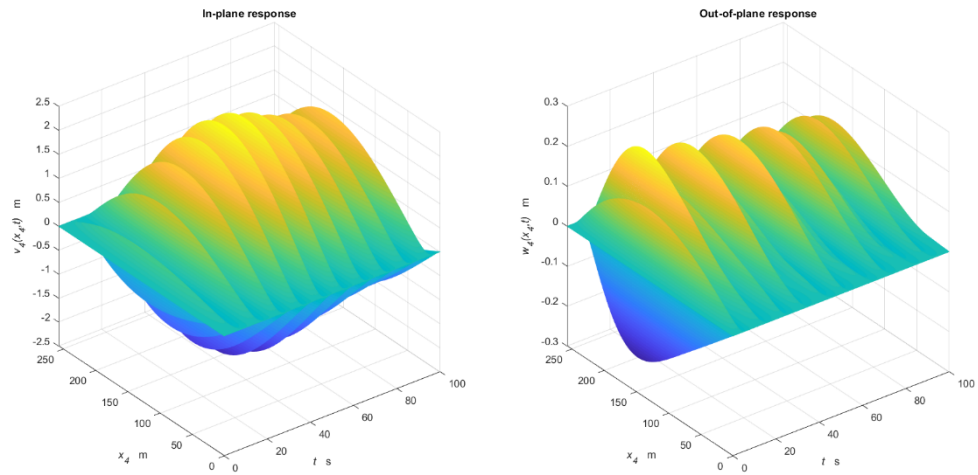


**Fig. 5** The response of compensating cables at the counterweight side

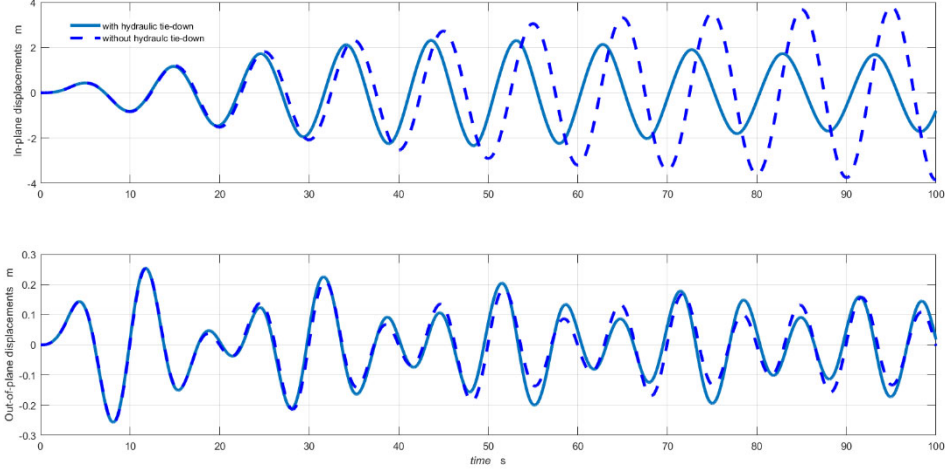


**Fig. 6** The maximum lateral displacements of compensating cables with the hydraulic tie-down (solid lines) and with no tie-down applied (dashed lines)

Following the methodology outlined above the PDE system Eq. 6 is discretized by using the Galerkin method so that the resulting set of nonlinear ordinary differential equations (ODE) can be simulated numerically. The simulated dynamic responses of the system for the scenario when the car is stationary at the level corresponding to the resonance length of  $L_4 = 257$  m of the compensating cables at the counterweight side ( $l_{car} = 45$  m, see Fig. 2) are presented in Figs 5 – 7, where the damping force given by Eq. 8 is determined for  $c_{comp} = 4.0 \times 10^5 \text{ N(m/s)}^{-0.3}$  ( $\alpha = 0.3$ ). Fig. 5 shows the in-plane and out-of plane dynamic displacements of the compensating cables at the counterweight side. The time records of the maximum lateral displacements of the cables (with the hydraulic tie-down and with no tie-down applied) and the vertical displacements are presented in Fig. 6 and Fig. 7, respectively. It is evident that the application of the hydraulic damper (tie-down) at the CSA results in the reduction of motions of the cables. The vertical response of the CSA is almost completely damped out whilst the vertical motions of the car are amplified.



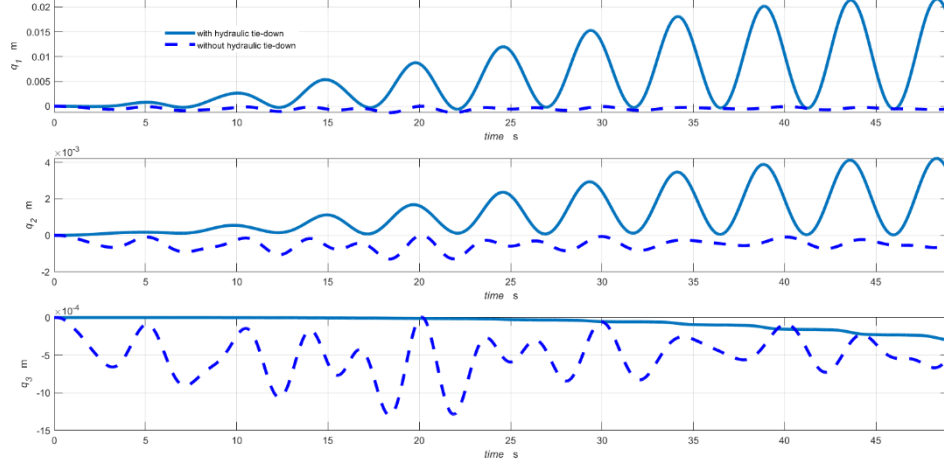


**Fig. 7** Vertical displacements of the car, counterweight and CSA, with the hydraulic tie-down (solid lines) and with no tie-down applied (dashed lines)

## 5 Active Control Strategy

The application of a passive hydraulic tie-down can be effective in reducing the resonance motions of the cables and vertical motions of the CSA. However, in practice this does not fully mitigate the effects of the resonance conditions. The resonance frequencies of the ropes can be shifted / changed using different masses of the CSA. The mass of the CSA can be increased or decreased in order to shift the resonance conditions. However, the dynamic conditions present in the building structure are such that even small changes in the natural frequencies of the structure might result in large changes of the resonance conditions. Thus, the potential effects of the application of passive control techniques and the resonance shifting strategy to achieve enough reduction the dynamic responses are limited.

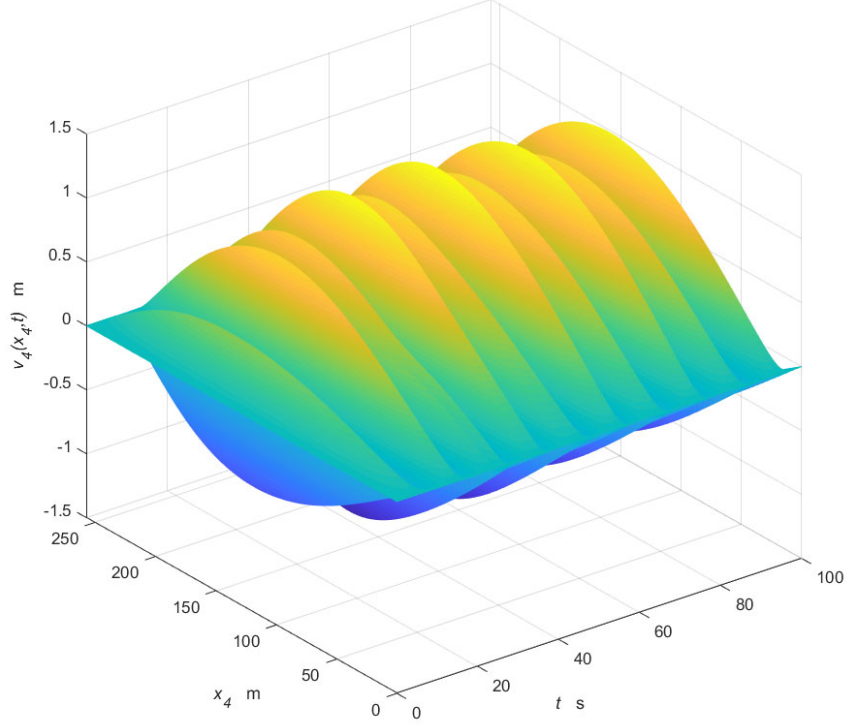


**Fig. 8** The response of compensating cables at the counterweight side with active control strategy applied

The active stiffness strategy can be sought to minimize the effects of adverse dynamic responses of suspension and compensating ropes in VTS [7]. To implement this strategy a servo-actuator is installed within the CSA tie-down system to control its vertical motion ( $q_3$ ). The motion of the CSA is then dictated by a suitable feedback control law. The following multimode feedback control law can be applied

$$q_3 \equiv u_{comp}(t) = a_u \frac{\sum_{n=1}^N q_n \dot{q}_n}{\sum_{n=1}^N \alpha_n^2 q_n^2} \quad (9)$$

where  $a_u$  is the control factor  $q_n$  represent the modes of the rope/ cable system and  $\alpha_n$  are the mode weighting coefficients. This law is implemented in the numerical simulation to demonstrate its effectiveness in reducing the resonance responses of the compensating ropes when the car position corresponds to the distance  $l_{car} = 45$  m. The active control is more effective than the passive damper / tie-down and results in a substantial reduction of the rope displacements, as demonstrated by the plots shown in figure 9. The control motion of the CSA (shown in black line) is generated by using the control factor  $a_u = 0.5$ . The FFT (Fast Fourier Transform) spectrum of the control signal is

shown in Fig. 10. The control law accommodates the in-plane as well as the out-plane modes to avoid the modal spill-over. The dominant frequency of the signal is 0.2 Hz which is twice the frequency of the fundamental resonance frequency of the cables.

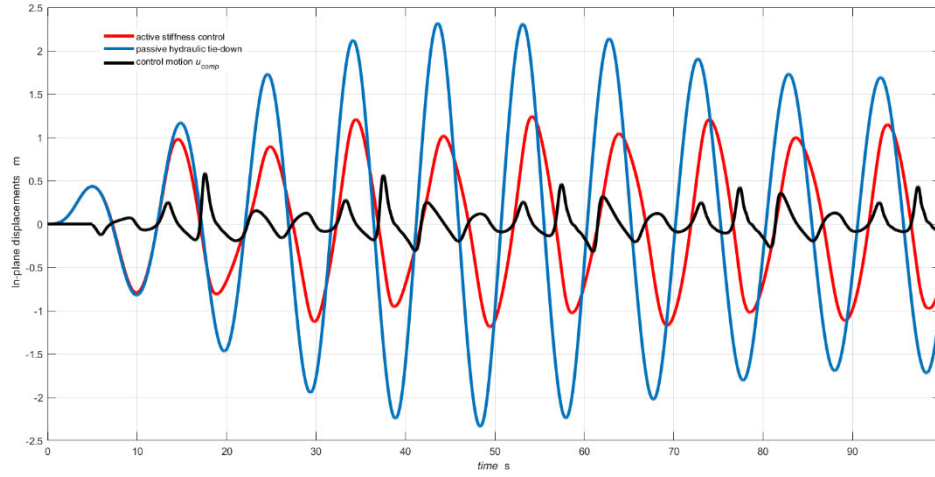


**Fig. 9** The maximum lateral displacements of compensating ropes with active stiffness and passive hydraulic damper / tie-down with the control motion shown

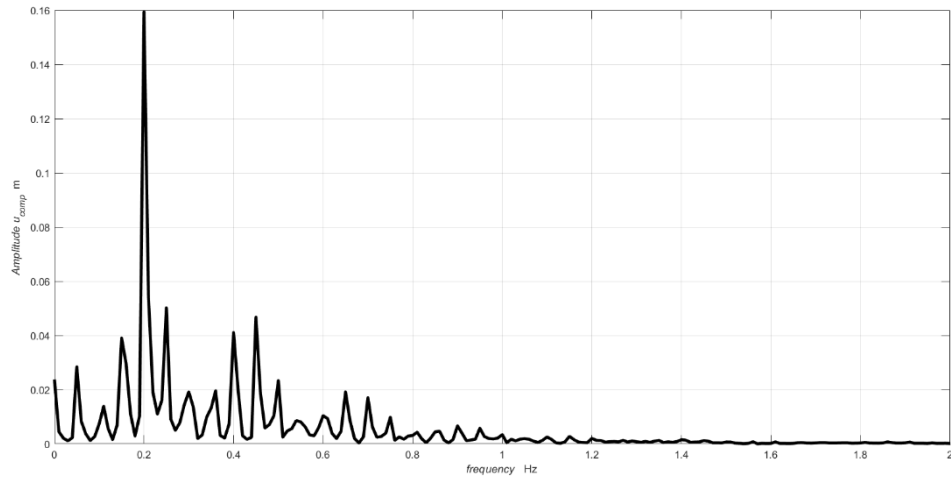


**Fig. 10** FFT spectrum of the control motion

## 6 Conclusion

Dynamic interactions that take place in VTS operating in high-rise structures result in adverse behaviour of their components compromising the structural integrity and safety of the installation. The application of passive hydraulic tie-down system at the CSA can mitigate the effects of fundamental resonances that occur in the compensating/ suspension cable systems. The study presented in this paper demonstrates that the active stiffness control is more effective. The case study demonstrates that when the proposed active control algorithm is used the response can be reduced by about 50% (in comparison with the response levels when the passive tie-down is applied).

## References

1. Kijewski-Correa T, Pirinia D.: Dynamic behavior of tall buildings under wind: insights from full-scale monitoring. *Struct. Des. Tall Spec.* **16**(4), 471-86 (2007)
2. Hu, R.P., Xu, Y.L., Zhao, X.: Long-period ground motion simulation and its impact on seismic response of high-rise buildings. *J. Earthq. Eng.* **22**(7), 1-31 (2018)
3. Kaczmarczyk, S.: The dynamics of vertical transportation systems: from deep mine operations to modern high-rise applications. In: Awrejcewicz, J., Kazmierczak, M., Mrozowski, J. and Olejnik, P. (eds.), *Dynamical Systems: Mechatronics and Life Sciences*. Lodz, Poland: Lodz University of Technology, 249-260 (2015)
4. Kaczmarczyk, S., Iwankiewicz, R.: Gaussian and non-Gaussian stochastic response of slender continua with time-varying length deployed in tall structures. *Int. J. Mech. Sci.* **134**, 500-510 (2017)
5. Crespo, R.S., Kaczmarczyk, S., Picton, P.D. Su, H.: Modelling and simulation of a stationary high-rise elevator system to predict the dynamic interactions between its components. *Int. J. Mech. Sci.* **137**, 24-45 (2018)
6. Kaczmarczyk, S.: The prediction and control of dynamic interactions between tall buildings and high-rise vertical transportation systems subject to seismic excitations. In: *The Proceedings of the 25th International Congress on Sound and Vibration (ICSV 25)*, Hiroshima, Japan, July 08-12 (2018)
7. Kaczmarczyk, S., Picton, P.D.: The prediction of nonlinear responses and active stiffness control of moving slender continua subjected to dynamic loadings in vertical host structures. *Int. J. of Acoust. Vib.* **18**(1), 39 – 44 (2013)
8. Mitropolskii, Y.A.: *Problems of the Asymptotic Theory of Nonstationary Vibrations*. Israel Program for Scientific Translations Ltd., Jerusalem (1965)
9. Kaczmarczyk, S.: The passage through resonance in a catenary – vertical cable hoisting system with slowly varying length. *J. Sound Vib.* **208**(2), 243 – 269 (1997)
10. Terumichi, Y., Ohtsuka, M., Yoshizawa, M., Fukawa, Y. and Tsujioka, Y.: Nonstationary vibrations of a string with time varying length and a mass-spring system at the lower end. *Nonlinear Dyn.* **12**, 39-55 (1997)
11. Sandilo, S.H. and Van Horssen, W.T.: On Variable Length Induced Vibrations of a Vertical String. *J. Sound Vib.* **333**(11), 2432-2449 (2013)
12. Sandilo, S.H. and Van Horssen, W.T.: On a cascade of autoresonances in an elevator cable system. *Nonlinear Dyn.* **80**, 1613-1630 (2015)
13. Gaiko, N.V. and Van Horssen, W.T. Resonances and vibrations in an elevator cable system due to boundary sway. *J. Sound and Vib.* **424**, 272-292 (2018)